

Photopolymerization Kinetics of Different Chain Sizes of Bi-functional Acrylic Monomers using Real Time FT-IR

Kentaro Taki^{1*}, Takehiro Taguchi², Ryota Hayashi¹, Hiroshi Ito²

¹*Chemical and Materials Engineering Course, School of Natural Systems, College of Science and Engineering, Kanazawa University, Kakumacho, Ishikawa 920-1192, Japan.*

²*Department of Polymer Science and Engineering, Yamagata University, 4-3-16, Jonan, Yonezawa, Yamagata, 992-8510, Japan*

In this study, the photopolymerization kinetics of bifunctional acrylic monomers having different chain lengths, such as 1,4-bis(acryloyloxy)butane, 1,6-bis(acryloyloxy)hexane, and 1,10-bis(acryloyloxy)decane, was investigated by real-time Fourier transform infrared (FTIR) spectroscopy, using Irgacure 184[®] (1 wt%) as the photoinitiator. Dark polymerization analysis was employed for measuring the kinetic constants for propagation and termination. Plots of kinetic constants for propagation against double-bond conversion showed a plateau, suggesting that the reaction rate is controlled at low conversion, and with increasing conversion, the reaction rate decreases as the diffusion rate of the monomer controls propagation. At low conversion, as compared to the reaction for a monomer having a long chain length, the propagation reaction for a monomer with a short chain length switched to a diffusion-rate controlled propagation reaction. The results suggested that short chain length monomers form a dense cross-linking network, which hinders the diffusion of the monomer, and the kinetic constants decrease at low conversion. The results obtained from the plot of kinetic chain length versus conversion indicated that at a maximum kinetic chain length of up to 10^6 , the reaction switches to the diffusion-rate controlled propagation of each monomer.

Keywords: free radical polymerization, photopolymerization, kinetics, FTIR

1. Introduction

UV curing or photopolymerization technology has been employed in a wide range of industries, such as electronics, cosmetics, construction, and printing. For designing a suitable formulation as well as UV curing process conditions, it is imperative to understand the kinetics of UV curing.

The UV-cured coating process involves bulk solvent-free cross-linking polymerization. The polymerization consists of photo-initiation, propagation, and termination reactions. After the photo-initiation occurred, the propagation occurs when the monomer approaches the primary or macro-radical. The propagation reaction proceeds ideally at low conversion that is reaction-rate controlled

propagation reaction. However, if the rate of diffusion of the monomer to the radical becomes slow with increase of conversion, as the cross-linking network hinders the diffusion of monomers, the propagation reaction rate is controlled by the diffusion rate of monomer [1].

The conversion at which the reaction-rate-controlled switches to the diffusion-rate-controlled corresponds to the onset of the formation of cross-linking networks. It is imperative to investigate the onset conversion for understanding the complex network structure formed by the photopolymerization of multi-functional monomers.

Numerical simulations of

photopolymerization are a powerful technique for analyzing UV curing, which has been investigated by several researchers [2-9].

Numerical simulations can be categorized into two approaches based on monomer diffusion. One of the approaches explicitly includes the diffusion of the monomer in the reaction-diffusion equation of the monomer [2]. The diffusion coefficient varies with double-bond conversion. However, it is difficult to experimentally determine diffusion-related parameters, such as mutual diffusion coefficient and attenuation factor.

The other approach includes the variation of the kinetic constants for propagation and termination with conversion [3,4,9]. The parameters in the models utilized in the aforementioned studies are determined by fitting the measured data of kinetic constants. The parameter fitting of the model significantly depends on initial values, and it is difficult to avoid local minimum convergence.

Moreover, the measured kinetic constants tend to change by the inhibition of oxygen and formation of cross-linking networks [9].

Although studies about network structure by measurements of the kinetic constants were reported so far [9-13], it is still challenging to investigate the kinetic of photopolymerization for elucidating the relationship between the photopolymerization kinetics and cross-linking network structures.

In this study, real-time Fourier transform infrared (FTIR) spectroscopy was employed for measuring the photopolymerization kinetics of bifunctional monomers having different chain lengths, such as 1,4-bis(acryloyloxy)butane, 1,6-bis(acryloyloxy)hexane, 1,10-bis(acryloyloxy)decane, using Irgacure 184[®] (1 wt%) as the photoinitiator. Dark polymerization analysis was employed for measuring the kinetic constants for propagation and termination.

2. Theory

Under UV irradiation, the dissociation of photoinitiator results in the continuous formation of its radicals, which readily react with the double bond, affording a primary radical; this primary radical then reacts with a monomer and forms macro-radicals. As a result, the monomer is consumed by the

radicals of the initiator as well as the primary radical and macro-radicals. Moreover, if the UV light is stopped, the photoinitiator is not dissociated, which in turn does not result in the production of initiator radicals. Hence, the monomer is consumed by either the primary or macro-radicals. Assuming that the primary radical is a part of macro-radical, their kinetic constants could be the same, determined as the kinetic constant for propagation k_p . The so-called dark polymerization has been employed for determining k_p and k_t , which has been thoroughly reviewed by Andrzejewska [13]. If bimolecular termination is considered for termination, two parameters, A and B , are determined by fitting to the conversion of experimental data as follows:

$$A = k_p / k_t \quad (1)$$

$$B = k_t [M_n^*]_0 \quad (2)$$

$$-\ln \frac{1-x_A(t)}{1-x_A(t_e)} = A \ln \{B(t-t_e)+1\} \quad (3)$$

$$\frac{k_p}{\sqrt{k_t}} [M]_0 (1-x_A) \sqrt{\eta I_0 \epsilon [PI]} = R_p \quad (4)$$

$$v = \frac{k_p [M]_0 (1-x_A(t_e)) [M_n^*]_0}{k_t [M_n^*]_0^2} \quad (5)$$

where k_p and k_t represent the kinetic constants for propagation and binary termination, respectively, $[M_n^*]_0$ represents the molar concentration of the macro-radical under UV light shut-off conditions, x_A represents the double-bond conversion, t represents the time, t_e represents the time under UV light shut-off conditions, $[M]_0$ represents the initial molar concentration of the double bond, η represents the quantum yield, I_0 represents the UV intensity at 365 nm, ϵ represents the molar absorption coefficient, $[PI]$ represents the photoinitiator concentration, R_p represents the polymerization rate under UV light shut-off conditions, and v represents the kinetic chain length.

3. Experimental

3.1. Materials

Bifunctional monomers, such as 1,4-bis(acryloyloxy)butane (**butane**, B2935), 1,6-bis(acryloyloxy)hexane (**hexane**, B2936), 1,10-bis(acryloyloxy)decane (**decane**, B2937) were purchased from Tokyo Chemical Industry (Japan). The monomer chain length increased in the order of **butane** < **hexane** < **decane**. Each monomer contained 25 ppm of

inhibitor MEHQ. The photoinitiator Irgacure 184[®] was purchased from BASF (Germany). All other reagents were used without further purification. The weight ratio of the monomer to photoinitiator was 99:1, and they were mixed for 1 h and stored in a refrigerator at 5 °C.

3.2. Real-time FTIR measurement

Two pieces of a $5 \times 5 \times 0.5^t$ mm³ KBr plate (JASCO, Japan) were used. A shim ring with a thickness of 10 μm, inner diameter ϕ of 3 mm, and outer diameter ϕ 5 mm was used. A sample plate was prepared as follows: First, a shim ring was placed on a KBr plate, and a drop of a monomer solution was dropped on the center of the shim ring. Second, another KBr plate was placed over the shim ring. The shim ring maintained the solution thickness constant for every measurement.

The sample plate was placed on a stage, which was maintained at 47 °C, of the optical bench of a real-time FTIR (VERTEX 70, Bruker-Optics, Germany) system. The beam from the beam splitter of the FTIR was transmitted to the normal direction of the sample plate. Simultaneously, the UV light was irradiated to the sample plate from an incident angle of 45°. The UV light was transmitted from a high-pressure mercury lamp (Omnicure[™] S2000, EXFO Co., Canada) through a liquid light guide. The UV intensity was measured by a photometer (UT-150, USHIO, Japan). The UV intensity was adjusted to 20 mW cm⁻² by changing the position of the liquid light guide and the iris of the lamp. The UV intensity was adjusted to a desired value within ± 0.1 mW cm⁻² for increasing reproducibility. A photodiode (GaAsP, G5842, Hamamatsu Photonics, Japan) was used to check if the UV light was on or off.

Typically, conversion is measured as follows: (1) UV intensity is adjusted using a UV meter. (2) The sample plate is placed on a temperature-controlled stage. (3) Real-time FTIR measurement is carried out under UV exposure. (4) UV light is switched off when the exposure time passes the pre-determined time. Real-time FTIR measurement was continued for 60 s for monitoring dark polymerization. The absorbance peak height at 812 cm⁻¹ was utilized for calculating conversion, and the wavenumber resolution was 8 cm⁻¹. Thirty-three spectra were recorded every 1 s. The details of the instrument and method have been reported

elsewhere [9].

Table 1 summarizes the parameters used for calculating the kinetic constants.

Table 1. Parameters for calculating kinetic constants.

Parameter	Value
UV intensity, I_0	6.1×10^{-5} Em ⁻² s ⁻¹ (20 mW cm ⁻²)
Absorption coefficient	0.966
Photoinitiator concentration	53.85 mol m ⁻³
Temperature	320.15 K
Molar concentration of the double bond	4.12 mol L ⁻¹

4. Results and Discussion

4.1. Conversion under UV light shut-off conditions

Fig. 1 shows the effect of irradiation time on the double-bond conversion under UV light shut-off conditions. Conversion increased with increasing irradiation time. In particular, conversion drastically increased until 2 s. At the same irradiation time, conversion followed the order of **decane** > **hexane** > **butane**. Difference in conversion was predominant for irradiation time greater than 1 s. Long chain length monomers exhibited high conversion.

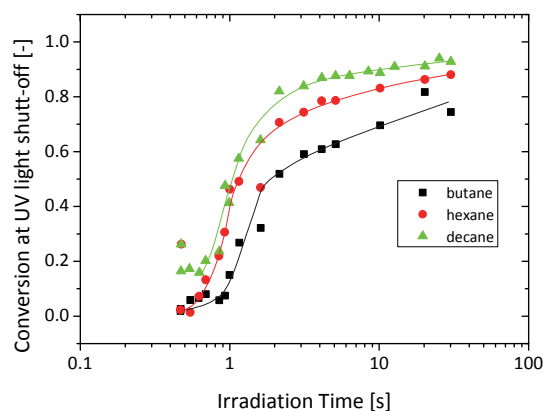


Fig. 1. Effect of irradiation time on conversion under UV light shut-off conditions. Temperature was 47 °C. UV intensity was 20 mW cm⁻². **butane**: 1,4-bis(acryloyloxy)butane, **hexane**: 1,6-bis(acryloyloxy)hexane, **decane**: 1,10-bis(acryloyloxy)decane.

Fig. 2 plots the kinetic constants for propagation k_p versus conversion. The plots of k_p vs. conversion exhibited a plateau at low conversion, and the kinetic constants decreased with increasing

conversion. The kinetic constant k_p of **butane** decreased at the lowest conversion of ~ 0.2 . The kinetic constant k_p of **hexane** decreased at a conversion of 0.5, and that of **decane** was 0.6. The kinetic constant of short chain length monomers decreased at low conversion. Short monomers are hypothesized to form dense networks, thereby switching to diffusion-rate-controlled polymerization at low conversion.

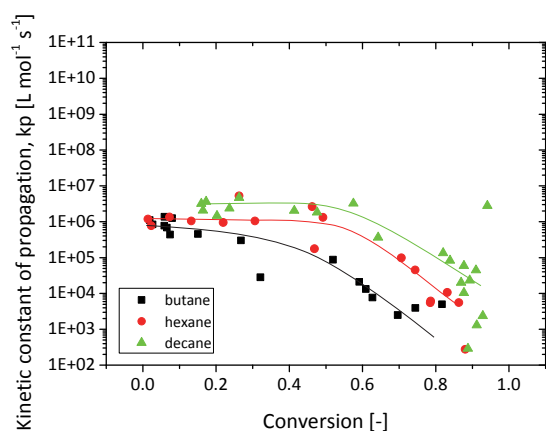


Fig. 2. Kinetic constant for propagation k_p versus conversion. The symbols used are the same as those shown in Fig. 1.

Fig. 3 shows the kinetic constant for termination k_t versus conversion. The plots of k_t decreased with increasing conversion. A plateau was not observed for the three monomers indicating that the termination reaction was controlled by the diffusion rate of radicals. As bimolecular termination occurred between two radicals, the majority of the radicals were trapped in the network. Hence, the kinetic constant for termination observed inherently includes the effect of the diffusion of radicals.

Fig. 4 plots kinetic chain length, representing the average number of monomer units consumed for each radical initiator that begins the polymerization of a chain, of each monomer versus conversion. Kinetic chain length varied with conversion. Interestingly, kinetic chain length exhibited a peak at around 1×10^6 at the conversion at which diffusion-rate-controlled polymerization started.

The kinetic chain grows in reaction-controlled polymerization. On the other hand, in diffusion-rate-controlled polymerization, the kinetic chain length does not propagate because of the limited diffusivity of monomers. Hence, the kinetic chain length attains a peak value.

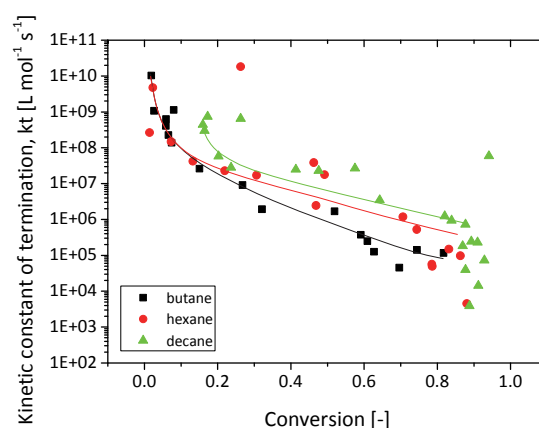


Fig. 3. Kinetic constants for termination k_t versus conversion. The symbols used are the same as those shown in Fig. 1.

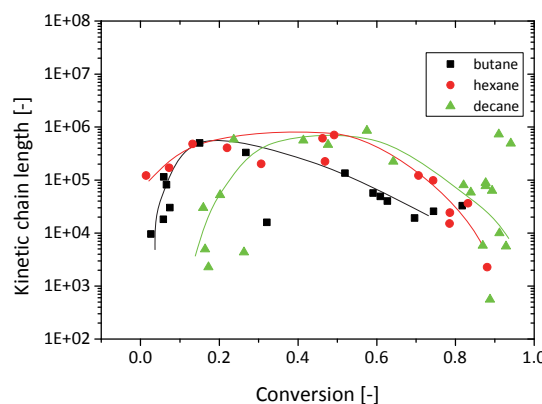


Fig. 4. Kinetic chain length versus conversion. The symbols used are the same as those shown in Fig. 1.

5. Conclusion

In this study, the photopolymerization kinetics of bifunctional monomers, such as 1,4-bis(acryloyloxy)butane, 1,6-bis(acryloyloxy)hexane, 1,10-bis(acryloyloxy)decane, with different chain lengths was investigated by real-time FTIR. Dark polymerization analysis was employed for measuring the kinetic constants for propagation and termination.

By the comparison of conversion among the three monomers at the same irradiation time, the longest monomer, 1,10-bis(acryloyloxy)decane, exhibited the highest conversion. The kinetic constant for propagation exhibited a plateau, indicating reaction-controlled polymerization. Then, the kinetic constant for propagation decreased with conversion, indicating diffusion-rate-controlled polymerization. The kinetic constant for propagation for the short chain

length monomer decreased at low conversion. The kinetic chain length exhibited a peak at the conversion of diffusion-rate-controlled polymerization.

References

1. D. L. Kurdikar, N. A. Peppas, *Macromolecules*, **27** (1994) 4084.
2. V. V. Krongauz, "Processes in Photoreactive Polymers", Edited by V. V. Krongauz and A. D. Trifunac, Chapman & Hall (1995) 185.
3. M. D. Goodner, H. R. Lee and C. N. Bowman, *Ind. Eng. Chem. Res.*, **36** (1997) 1247.
4. M. D. Goodner and C. N. Bowman, *Chem. Eng. Sci.*, **57** (2002) 887.
5. D. Dendukuri, P. Panda, R. Haghgoie, J. M. Kim, T. A. Hatton and P. S. Doyle, *Macromolecules*, **41** (2008) 8547.
6. Y. Zhang, D. E. Kranbuehl, H. Sautereau, G. Seytre and J. Dupuy, *Macromolecules*, **42** (2009) 203.
7. G. A. Altun-Çiftçioğlu, A. Ersoy-Meriçboyu and C. L. Henderson, *Polym. Eng. Sci.*, **51** (2011) 1710.
8. A. S. Jariwala, F. Ding, A. Boddapati, V. Breedveld, M. A. Grover, C. L. Henderson and D. W. Rosen, *Rapid Prototyping J.*, **17** (2011) 168.
9. K. Taki, Y. Watanabe, H. Ito and M. Ohshima, *Macromolecules*, **47** (2014) 1906.
10. K. S. Anseth and C. N. Bowman, *Polym. React. Eng.*, **1** (1992-93) 499.
11. K. S. Anseth, C. M. Wang, C. N. Bowman, *Polymer*, **35** (1994) 3243.
12. K. S. Anseth, C. M. Wang, C. N. Bowman, *Macromolecules*, **27** (1994) 650.
13. E. Andrzejewska, *Prog. Polym. Sci.*, **26** (2001) 605.